

$N\bar{N} \rightarrow 3\pi$ amplitudes and the symmetric-group dual resonance model*

A. Nandy, P. H. Frampton, and T. E. Kalogeropoulos
 Department of Physics, Syracuse University, Syracuse, New York 13210
 (Received 31 October 1974)

Annihilation processes $N\bar{N} \rightarrow 3\pi$ are compared to a suitably adapted symmetric-group dual resonance model for pion-pion elastic scattering in which the over-all normalization is the only free parameter. The fits are found to be rather unsuccessful, essentially because of the absence of odd daughter trajectories, and it is shown that there is no way of obtaining a better result from this model, even by the usual artifice of completely eliminating the ρ trajectory.

The reaction

$$\bar{p}n \rightarrow \pi^+ \pi^- \pi^- \text{ at rest} \quad (1)$$

has been explained by the Veneziano model¹ to a satisfactory degree such that it has become a standard test case for any four-pion dual amplitude. The first successful explanation for the three-pion Dalitz plot for this reaction² was given by Lovelace,³ who observed that the $\bar{p}n$ state has the quantum numbers ($J^P = 0^-$) of a heavy pion, so that the process could be related to a $\pi\pi$ scattering amplitude. Considering the lack of a strong ρ band, he proposed an amplitude,

$$A(s, t) = \frac{\Gamma(1 - \alpha(s))\Gamma(1 - \alpha(t))}{\Gamma(2 - \alpha(s) - \alpha(t))} \quad (2)$$

with

$$\alpha(x) = 0.483 + 0.885x + 0.280i(x - m_\pi^2)^{1/2} \quad (3)$$

(where s is the four-momentum squared of π^+ and

π_1^- , t is that of π^+ and π_2^- , and m_π is the pion mass), which was able to account, at least qualitatively, for the two most striking features of this Dalitz plot: (i) a strong enhancement in the low ($\pi^-\pi^-$) mass region and (ii) a large area of depletion of events in the center of the plot where $M^2(\pi^+\pi_1^-) = M^2(\pi^+\pi_2^-) \approx 1.08 \text{ GeV}^2$. Earlier efforts at explaining these features by superimposing resonances had not met with much success, even when a strong exotic ($\pi^-\pi^-$) contribution was included.²

However, the Lovelace fit, although spectacular, was not accurate in detail—for example, the hole at the center of the Dalitz plot was not as well defined as demanded by the data—and this led to several attempts^{4,5} to improve the agreement by adding satellite terms or changing the imaginary part of the trajectory function.⁶ Since the zero of Eq. (2) coming from the pole of the Γ function at $\alpha(s) + \alpha(t) = 3$ is important to the fit, Altarelli and Rubinstein⁴ generalized Eq. (2) to the form

$$A(s, t) = C_{10} \frac{\Gamma(1 - \alpha(s))\Gamma(1 - \alpha(t))}{\Gamma(1 - \alpha(s) - \alpha(t))} + C_{11} \frac{\Gamma(1 - \alpha(s))\Gamma(1 - \alpha(t))}{\Gamma(2 - \alpha(s) - \alpha(t))} + C_{20} \frac{\Gamma(2 - \alpha(s))\Gamma(2 - \alpha(t))}{\Gamma(2 - \alpha(s) - \alpha(t))} + C_{21} \frac{\Gamma(2 - \alpha(s))\Gamma(2 - \alpha(t))}{\Gamma(3 - \alpha(s) - \alpha(t))} + C_{30} \frac{\Gamma(3 - \alpha(s))\Gamma(3 - \alpha(t))}{\Gamma(3 - \alpha(s) - \alpha(t))} \quad (4)$$

and got a better fit to the projections of the plot by adjusting the coefficients. The essential two-dimensional nature of the problem, however, was pointed out by Gopal, Migneron, and Rothary, who were able to obtain an excellent fit over the whole Dalitz plot by a more careful consideration of the coefficients of the satellite terms in Eq. (4).

Recently, a new type of dual resonance model has been proposed.⁷ Its construction is based on the use of the symmetric group, and it provides for four pseudoscalar mesons a Born amplitude of the form

$$A_4(s, t) = \int_0^1 dx x^{-\alpha(t)-1} (1-x)^{-\alpha(s)-1} \times [(x - e^{i\pi/3})(x - e^{-i\pi/3})]^{\gamma/2} \times \phi_4(\alpha(s), \alpha(t), \alpha(u); x), \quad (5)$$

where

$$\gamma = 1 + \alpha(s) + \alpha(t) + \alpha(u) \quad (6)$$

and

$$\begin{aligned} \phi_4(\alpha(s), \alpha(t), \alpha(u); x) \\ = (1-x+x^2)^{-1} [\alpha(s)x + \alpha(t)(1-x) - \alpha(u)x(1-x)]. \end{aligned} \quad (7)$$

This model, which has no odd daughter trajectories, preserves all requirements of analyticity, crossing symmetry, and Regge behavior, provides room for generalization to N -point functions, and includes several earlier generalized Euler B -function models as special cases.⁸ It has also been suggested that the amplitude in Eq. (5) can be derived from a factorizable ghost-free scheme even for physical intercepts such as $\alpha_\rho(0) = \frac{1}{2}$; this is a major theoretical advantage over the old Lovelace formula.

Although the amplitude in Eq. (5) was originally proposed for pion-pion scattering, it is natural to test it phenomenologically in the annihilation process. We have considered two reactions: (i) $\bar{p}n \rightarrow \pi^+\pi^-\pi^-$, where the amplitude is given by $A_4(s, t)$, and (ii) the reaction

$$\bar{p}p \rightarrow \pi^0\pi^0\pi^0 \text{ at rest,} \quad (8)$$

where symmetry dictates that the amplitude be $[A_4(s, t) + A_4(t, u) + A_4(u, s)]$; in both cases, the only free parameter in the problem is the over-all normalization. We use the same trajectory function as Lovelace [Eq. (3)]. The amplitude A_4 is evaluated by expanding into a finite series of B functions plus a remainder integral, which is evaluated numerically.

We have obtained fits for the two reactions over the two-dimensional Dalitz plot. The method used⁹

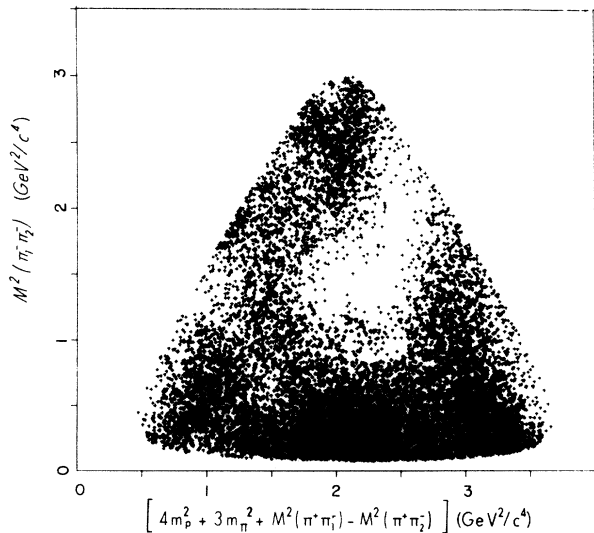


FIG. 1. Comparison of experiment and the symmetric-group model for the reaction $\bar{p}n \rightarrow \pi^+\pi^-\pi^-$ at rest. The experimental data are on the left half of the plot and the symmetric-group model predictions on the right.

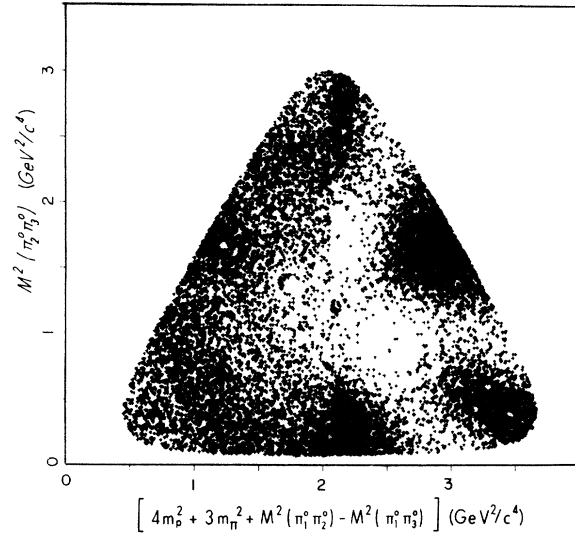


FIG. 2. Comparison of experiment and the symmetric-group model for $\bar{p}p \rightarrow 3\pi^0$ at rest. The experimental data are on the left half of the plot and the model predictions on the right.

consists of dividing a part of the Dalitz plot into a number of bins of equal areas, calculating the contribution of the new amplitude to each bin, and then using a random-number routine to generate events of the required density. The results are shown in Figs. 1-3, in each of which the left half shows the experimental data.^{2,10} Figure 1 is for the reaction $\bar{p}n \rightarrow \pi^+\pi^-\pi^-$ and the results of the new model (the Lovelace model is discussed elsewhere⁹); Figs. 2 and 3 are for $\bar{p}p \rightarrow \pi^0\pi^0\pi^0$ compared

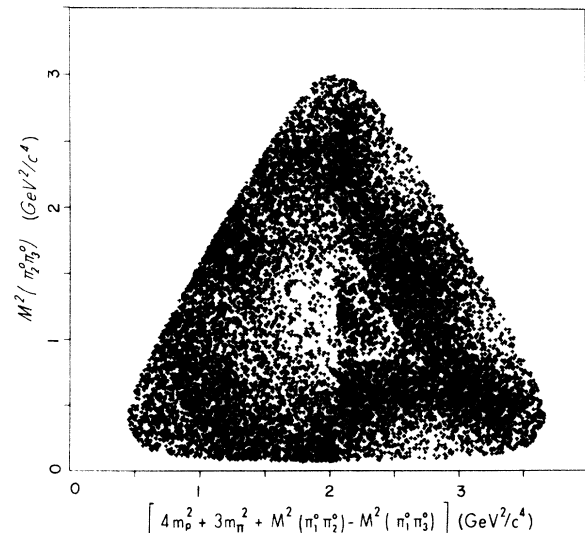


FIG. 3. Comparison of experiment and the Lovelace model for $\bar{p}p \rightarrow 3\pi^0$ at rest. The experimental data are on the left half of the plot and the model predictions on the right.

to the new model and Lovelace's amplitude, respectively. The fits are clearly unsatisfactory. Table I lists the χ^2 values.

The fit to $\bar{p}n \rightarrow 2\pi^- \pi^+$ reproduces the two prominent features of the experimental data—viz., the low-mass $\pi^- \pi^-$ enhancement and the central hole—but is otherwise generally unsuccessful. The failure of this model is, however, rather instructive: The essential point is that the symmetric-group model we have used, unlike the Lovelace model and its extensions, contains no odd daughter trajectories.⁷ Thus, in the region of $\alpha(s), \alpha(t) = 1$ there is only a spin-one ρ resonance without any s wave, and the residues there, being proportional to $\cos\theta$ where θ is the scattering angle, must vanish at $\theta = \pi/2$. Hence there is a marked depletion of events at $\alpha_s = 1$ near $t = u$ and at $\alpha_t = 1$ near $s = u$. Experimentally, the $\alpha_\rho = 1$ bands show approximate isotropy, and this is generally cited as evidence that the ρ is only very weakly produced in the annihilation process.²

The Lovelace procedure of summarily rejecting the ρ trajectory will not work here for at least two reasons.

(i) If we consider using an amplitude

$$A(s, t) = \int_0^1 dx x^{-\alpha_t-1} (1-x)^{-\alpha_s-1} \times (1-x+x^2)^{(\alpha_s+\alpha_t+\alpha_u-1)/2}, \quad (9)$$

where the leading trajectory has the intercept $\alpha(0) = \alpha_\rho(0) - 1$, then compared to $\pi\pi \rightarrow \pi\pi$ we have only odd daughters and the resonances in $\pi\pi \rightarrow \pi\pi$ and $(\bar{p}n) \rightarrow 3\pi$ become nonoverlapping sets.

(ii) If nevertheless we *do* use Eq. (9), then although the residues at unit $\alpha_\rho(s)$ and $\alpha_\rho(t)$ are satisfactory the residues at $\alpha_\rho(s) = 2$ and $\alpha_\rho(t) = 2$ become unsatisfactory since they contain only spin-one (ρ') resonances and consequently vanish at $\theta = \pi/2$, contrary to experiment.

The fits to $\bar{p}p \rightarrow 3\pi^0$ by the symmetric-group and Lovelace models also show poor agreements. Since the symmetric-group model has only evenly

TABLE I. χ^2 values obtained by fitting the Lovelace and symmetric-group-model amplitudes for the reactions $\bar{p}n \rightarrow \pi^+ \pi^- \pi^-$ and $\bar{p}p \rightarrow \pi^0 \pi^0 \pi^0$ at rest.

Reaction	Amplitude	χ^2	No. of bins
$\bar{p}n \rightarrow \pi^+ \pi^- \pi^-$	Lovelace ⁹	2457	300
	at rest Symmetric group	2754	300
$\bar{p}p \rightarrow \pi^0 \pi^0 \pi^0$	Lovelace	1108	100
	at rest Symmetric group	1424	100

spaced trajectories, the symmetry of the problem implies the presence of a dominant f^0 resonance and a residue proportional to $\cos^4\theta$; this gives the sharp enhancements at the low $2\pi^0$ mass region and the wide areas of depletion in between (Fig. 2). The Lovelace model, on the other hand, has the ϵ trajectory and produces a strong band structure for the ϵ but a very weak enhancement at the low $2\pi^0$ mass region, presumably because the spin-zero ϵ would be the dominant member.

The failures of these fits are disappointing. The best fits have been obtained by fitting coefficients of Eq. (4). The motivation of the present work was not only to test a new model in a new context, but also, because of the unique feature, among others, that there are no parameters in this model, to understand the origin of these coefficients. The hole at the center of the Dalitz plot and the low-mass $\pi\pi$ enhancement are gross features that are successfully predicted by essentially any dual model parametrization, but dual models have given no understanding of the relative strengths of the final-state resonances. In particular, our present results draw renewed interest to a long-standing mystery of why the ρ meson is not produced with normal strength in $\bar{p}n \rightarrow (2\pi^-)\pi^+$.

We would like to thank Dr. A. P. Balachandran for useful discussions on this subject.

*Work supported in part by the National Science Foundation.

¹G. Veneziano, Nuovo Cimento **57A**, 190 (1968).

²P. Anninos, L. Gray, P. Hagerty, T. Kalogeropoulos, S. Zenone, R. Bizzarri, G. Ciapetti, M. Gaspero, I. Laakso, S. Lichtman, and G. C. Moneti, Phys. Rev. Lett. **20**, 402 (1968).

³C. Lovelace, Phys. Lett. **28B**, 264 (1968).

⁴G. Altarelli and H. R. Rubinstein, Phys. Rev. **183**, 1469 (1969).

⁵G. P. Gopal, R. Migneron, and A. Rothery, Phys. Rev. D **3**, 2262 (1971). See also H. R. Rubinstein, E. J. Squires, and M. Chaichian, Phys. Lett. **30B**, 189 (1969); S. Pokorski, R. O. Ratio, and G. H. Thomas,

Nuovo Cimento **7A**, 828 (1972); R. Odorico, Phys. Lett. **33B**, 489 (1970).

⁶C. Boldrighini and A. Pugliese, Nuovo Cimento Lett. **2**, 239 (1969).

⁷P. H. Frampton, Phys. Rev. D **7**, 3077 (1973).

⁸For a detailed discussion of these and other aspects of this model, see P. H. Frampton, *Dual Resonance Models* (Benjamin, New York, 1974).

⁹T. E. Kalogeropoulos, A. Nandy, and J. Roy (unpublished).

¹⁰S. Devons, T. Kozlowski, P. Nemethy, S. Shapiro, M. Dris, N. Horowitz, T. Kalogeropoulos, J. Skelly, R. Smith, and H. Uto, Phys. Lett. **47B**, 271 (1973).

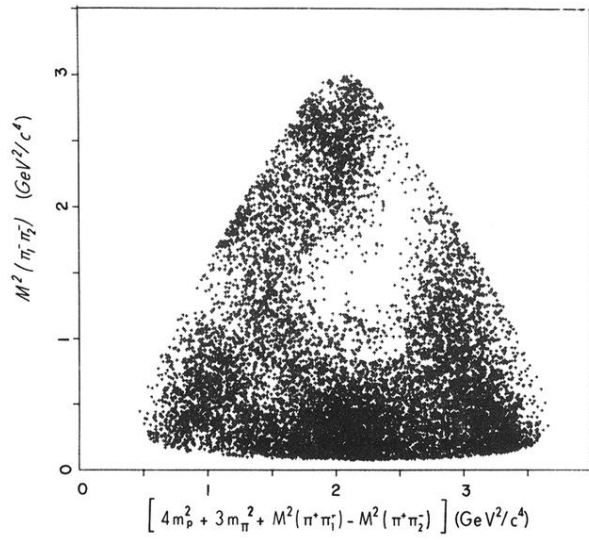


FIG. 1. Comparison of experiment and the symmetric-group model for the reaction $\bar{p}n \rightarrow \pi^+\pi^-\pi^-$ at rest. The experimental data are on the left half of the plot and the symmetric-group model predictions on the right.

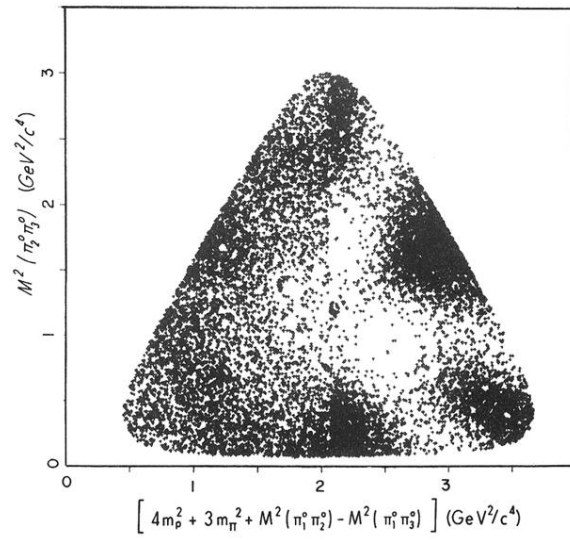


FIG. 2. Comparison of experiment and the symmetric-group model for $\bar{p}p \rightarrow 3\pi^0$ at rest. The experimental data are on the left half of the plot and the model predictions on the right.

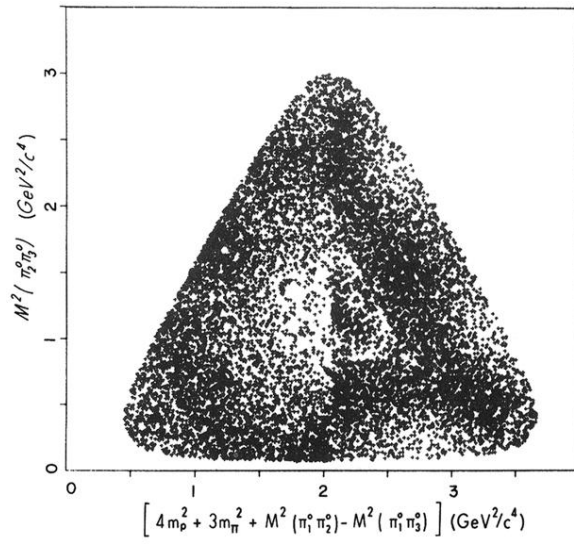


FIG. 3. Comparison of experiment and the Lovelace model for $\bar{p}p \rightarrow 3\pi^0$ at rest. The experimental data are on the left half of the plot and the model predictions on the right.